10.1098/rspa.2001.0868

THE ROYAL SOCIETY

The initial boundary problem for the Korteweg–de Vries equation on the negative quarter-plane

By T. R. Marchant[1] and N. F. Smyth[2]

[1]*School of Mathematics and Applied Statistics, The University of Wollongong, Wollongong, 2522 NSW, Australia*
[2]*Department of Mathematics and Statistics, University of Edinburgh, The King's Buildings, Mayfield Road, Edinburgh EH9 3JZ, UK*

Received 20 March 2001; accepted 23 July 2001; published online 18 February 2002

The initial boundary-value problem for the Korteweg–de Vries (KdV) equation on the negative quarter-plane, $x < 0$ and $t > 0$, is considered. The formulation of this problem is different to the usual initial boundary-value problem on the positive quarter-plane, for which $x > 0$ and $t > 0$. Two boundary conditions are required at $x = 0$ for the negative quarter-plane problem, in contrast to the one boundary condition needed at $x = 0$ for the positive quarter-plane problem. Solutions of the KdV equation on the infinite line, such as the soliton, cnoidal wave, mean height variation and undular bore solution, are used to find approximate solutions to the negative quarter-plane problem. Five qualitatively different types of solution are found, depending on the relation between the initial and boundary values. Excellent comparisons are obtained between these solutions and full numerical solutions of the KdV equation.

Keywords: KdV equation; modulation theory; initial boundary-value problems

1. Introduction

The Korteweg–de Vries (KdV) equation is the generic equation for the study of weakly nonlinear long waves. It arises in physical systems which involve a balance between weak nonlinearity and weak dispersion at leading order (Whitham 1974). The KdV equation arises in many physical situations, such as surface water waves, internal waves in a density-stratified fluid, plasma waves, Rossby waves and magma flow. The KdV equation is integrable and can be solved on the infinite line using the so-called inverse scattering transform (Gardner *et al.* 1967). The inverse scattering solution shows that when a larger KdV solitary wave overtakes a smaller one, both the solitary waves retain their original shapes, with the only memory of the collision being a phase shift. Due to this special, particle-like property, amongst others, the solitary-wave solution of the KdV equation is termed a soliton. The explicit solution for interacting KdV solitons was developed using inverse scattering by Hirota (1972). The initial boundary-value (IBV) problem for the KdV equation has been considered

by a number of authors. It can be written as

$$\left.\begin{aligned} \frac{\partial u}{\partial t} + 6u\frac{\partial u}{\partial x} + \frac{\partial^3 u}{\partial x^3} &= 0, & x &> 0, \\ u(x,0) &= u_{\mathrm{i}}(x), & x &> 0, \\ u(0,t) &= u_{\mathrm{b}}(t), & t &> 0, \end{aligned}\right\} \tag{1.1}$$

and is commonly referred to as the quarter-plane problem, since $x > 0$ and $t > 0$. A number of physical applications exist for (1.1), such as the generation of waves in a shallow channel by a wave-making device or the critical withdrawal of a stratified fluid from a reservoir (Clarke & Imberger 1994).

Chu *et al.* (1983) considered the positive quarter-plane problem (1.1) numerically. The energy conservation law for the KdV equation was used to deduce that one boundary condition should be applied at $x = 0$, with the other two being boundedness conditions on the solution as $x \to \infty$. For their examples, a train of solitons was generated at the boundary and it was found that the soliton amplitudes were related to the boundary condition by a simple formula. It was also shown that the addition of a damping term in the KdV equation led to a steady collisionless shock being generated. Fokas & Ablowitz (1989) examined (1.1) using inverse scattering, which reduced the problem to that of a nonlinear singular integro-differential equation for the scattering data. Camassa & Wu (1989) found approximate solutions to (1.1) by using inverse scattering and assuming values for u_x and u_{xx} at the boundary $x = 0$. Both trapezoidal and exponentially decaying functions were used for the time-varying boundary condition u_{b}. Their approximate method gave a reasonable estimate for the soliton amplitudes (within 20%) for large amplitudes. However, it was unable to accurately estimate the amplitudes of small solitons. A drawback to their method is that the values of u_x and u_{xx} are generally not known *a priori*.

Fokas (1997) developed a new transform method for solving IBV problems for linear and integrable nonlinear partial differential equations, based on the fact that these types of equations possess a Lax pair. The resulting spectral analysis allows the solution to be represented in a simple integral form. Examples considered include the NLS and sine-Gordon equations, and their respective linearized versions. Moreover, it was found that the boundary and initial conditions must satisfy a certain global constraint for the IBV problem to be well-posed. Fokas & Pelloni (1998) used this transform method to solve a number of IBV problems for the linearized KdV equation. Quarter-plane and wedge-shaped domains with both Dirichlet and Neumann boundary conditions were examined. The solution of the nonlinear KdV equation was also discussed, but not undertaken. Fokas & Pelloni (2000) solved a linear dispersive equation, of general form, on a time-dependent boundary, again using the transform method. The interested reader is referred to the review paper by Fokas (2000) for more details and applications of the transform method.

Marchant & Smyth (1991) also considered the quarter-plane problem (1.1) and found approximate and exact solutions. For the case of constant boundary and initial conditions, various types of steady and transient solutions were derived, the particular form of the solution depending on the relationship between u_{b} and u_{i}. In addition, a case was considered of a time-dependent boundary condition u_{b}, for which an approximate solution was derived using modulation theory for the KdV equation (Whitham 1974) and the fact that the solution consisted of a train of solitons. For all the cases considered, excellent comparisons were obtained between the

approximate solutions and numerical solutions of (1.1). Clarke & Imberger (1994) considered the critical withdrawal of a two-layer fluid via a sink as a model for the withdrawal of water from a reservoir. The case of critical withdrawal corresponds to when the upper layer is just drawn into the sink. The problem was formulated as an IBV problem for the KdV equation and the solutions of Marchant & Smyth (1991) were used to show that three different withdrawal regimes exist. These were uniform withdrawal, when fluid is drawn from both layers, selective withdrawal, when water is drawn from the lower layer only, and a case termed partial withdrawal.

In the present paper the negative quarter-plane problem for $x < 0$ and $t > 0$ will be examined. This problem can be stated as

$$\left.\begin{aligned} \frac{\partial u}{\partial t} + 6u\frac{\partial u}{\partial x} + \frac{\partial^3 u}{\partial x^3} &= 0, & x < 0,\\ u(x,0) &= u_{\mathrm{i}}(x), & x < 0,\\ u(0,t) &= u_{\mathrm{b}}(t), & t > 0,\\ \frac{\partial u(0,t)}{\partial x} &= u_{\mathrm{b}x}(t), & t > 0. \end{aligned}\right\} \tag{1.2}$$

In the present work, only the case of constant initial and boundary conditions will be considered, so that u_{i}, u_{b} and $u_{\mathrm{b}x}$ are all constants. The negative quarter-plane problem is of interest for a number of reasons. Firstly, its mathematical formulation is different from the positive quarter-plane problem (1.1), as the number of boundary conditions needed at $x = 0$ is different. This leads to solutions for the negative quarter-plane problem being different to those for the positive quarter-plane problem. Secondly, it is related to the problem on the positive quarter-plane when the dispersive term in the KdV equation has a negative coefficient. Applying the transformation $x \to -x$ and $u \to -u$ to the negative quarter-plane problem (1.2) gives the problem on the positive quarter-plane for the KdV equation

$$\frac{\partial u}{\partial t} + 6u\frac{\partial u}{\partial x} - \frac{\partial^3 u}{\partial x^3} = 0. \tag{1.3}$$

One physical example for which (1.3) is appropriate is weakly nonlinear long waves propagating on a fluid with surface tension. The coefficient of the dispersive term becomes negative if the Bond number τ, which measures the magnitude of the surface tension, is greater than one-third (Kichenassamy & Olver 1992). The paper is organized as follows. Section 2 discusses the various exact and approximate solutions of the KdV equation on the infinite-line which are needed to construct solutions for the negative quarter-plane problem. In § 3 the linear KdV equation is used to illustrate and justify the number of boundary conditions needed at $x = 0$ for both the positive and negative quarter-plane problems. Then the various solutions of § 2 are used to construct approximate solutions for the negative quarter-plane problem (1.2). In § 4 the approximate solutions of (1.2), found in § 3, are compared with numerical solutions of the KdV equation. The appendix provides details of the numerical scheme used.

2. Solutions of the Korteweg–de Vries equation

In this section some solutions of the KdV equation on the infinite line, $-\infty < x < \infty$, are presented and discussed. These solutions will be used in § 3 to find analytical solutions of the negative quarter-plane problem (1.2).

A particular solution of the KdV equation is the cnoidal wave solution (Whitham 1974),

$$u = \beta + 2a\left[m^{-1} - 1 - m^{-1}P(m) + \mathrm{cn}^2\left(\frac{K(m)\theta}{\pi}\right)\right], \tag{2.1}$$

where the phase θ, wavenumber k and dispersion relation ω are

$$\left.\begin{aligned} \theta &= kx - \omega t + \phi, \\ k &= \frac{\pi}{K(m)}\sqrt{\frac{a}{m}}, \\ \omega &= 6\beta k + 4ak(2m^{-1} - 1 - 3m^{-1}P(m)). \end{aligned}\right\} \tag{2.2}$$

Here cn is the Jacobian elliptic cosine function of parameter (modulus squared) m. $P(m)$ is defined as the ratio

$$P(m) = \frac{E(m)}{K(m)}, \tag{2.3}$$

where $K(m)$ and $E(m)$ are complete elliptic integrals of the first and second kinds, respectively. The mean height of the cnoidal wave (2.1) is β and its amplitude is a. A special case (for $m = 1$) of the cnoidal wave solution (2.1) is the soliton solution

$$u = \beta + 2a\,\mathrm{sech}^2\sqrt{a}[x - (6\beta + 4a)t + \phi]. \tag{2.4}$$

Many of the solutions of the next section for the IBV problem (1.2) will be based on modulation theory for the KdV equation, which was derived by Whitham (1965, 1974). Modulation theory assumes that the amplitude, mean height and wavenumber of the cnoidal wave (2.1) are slowly varying functions of x and t. Based on an averaged Lagrangian technique, Whitham (1965, 1974) showed that the modulation equations governing the evolution of these parameters form the third-order hyperbolic system

$$\left.\begin{aligned} &\text{P:}\quad 2\beta + 4am^{-1}(1 - P(m)) - 2a - 2am^{-1} = \text{const.} \\ &\qquad\qquad \text{on } \frac{\mathrm{d}x}{\mathrm{d}t} = U - \frac{4a}{1 - P(m)}, \\ &\text{Q:}\quad 2\beta + 4am^{-1}(1 - P(m)) - 2am^{-1} = \text{const.} \\ &\qquad\qquad \text{on } \frac{\mathrm{d}x}{\mathrm{d}t} = U - \frac{4a(1-m)}{P(m) - (1-m)}, \\ &\text{R:}\quad 2\beta + 4am^{-1}(1 - P(m)) - 2a = \text{const.} \\ &\qquad\qquad \text{on } \frac{\mathrm{d}x}{\mathrm{d}t} = U + \frac{4a(1-m)}{mP(m)}, \end{aligned}\right\} \tag{2.5}$$

where the phase velocity and wavenumber of the modulated cnoidal wavetrain are

$$U = 6\beta + 4a(2m^{-1} - 1 - 3m^{-1}P(m)), \qquad k = \frac{\pi}{K(m)}\sqrt{\frac{a}{m}}. \tag{2.6}$$

The modulation equations (2.5) have a simple wave solution, whose physical interpretation is an undular bore. This solution was first derived by Gurevich & Pitaevskii (1974) and Fornberg & Whitham (1978). The simple wave solution is formed as an

expansion fan on the characteristic Q, which links a level A ahead of the bore to a level B behind the bore, for $B > A$. In detail this simple wave, or undular bore, solution is

$$\left.\begin{aligned}\beta &= (B-A)m + 2A - B + 2(B-A)P(m),\\ a &= (B-A)m,\\ k &= \frac{\pi}{K(m)}(B-A)^{1/2},\end{aligned}\right\} \tag{2.7}$$

on

$$\frac{x}{t} = 2(B-A)m + 4A + 2B - \frac{4(B-A)m(1-m)}{P(m)-(1-m)},$$
$$12A - 6B \leqslant \frac{x}{t} \leqslant 4B + 2A, \quad 0 \leqslant m \leqslant 1. \tag{2.8}$$

At the front of the bore the mean level $\beta = A$. At this leading edge $m = 1$ and solitons of amplitude $2(B-A)$ occur. At the rear of the bore, where $m = 0$, the mean level $\beta = B$ and sinusoidal waves of small amplitude occur. As $B > A$, this bore represents a step up in mean height from the front to the rear of the bore. Another solution of the KdV equation which will be used in the present work is

$$u = \frac{x}{6t}, \quad 6Bt \leqslant x \leqslant 6At, \tag{2.9}$$

with $u = A$ for $x > 6At$ and $u = B$ for $x < 6Bt$, so that the mean levels ahead of and behind the expansion wave (2.9) are A and B, respectively. This solution is valid for $B < A$, so is the resolution of a step down in mean height, in contrast to the undular bore solution (2.7), which is the resolution of a step up in mean height. Fornberg & Whitham (1978) found both the undular bore solution (2.7) and the mean height variation (2.9) to be in excellent agreement with numerical solutions of the KdV equation on the infinite line for step initial conditions.

3. Solutions of the initial boundary-value problem

The solutions (2.1), (2.4) and (2.7)–(2.9) of the KdV equation on the infinite line will now be used to determine solutions of the negative quarter-plane problem (1.2). These solutions will be compared with numerical solutions of the KdV equation in the next section. The specific form of the solution of the negative quarter-plane problem depends on the relation between the values of u_i, u_b and $u_{\mathrm{b}x}$. Before calculating these solutions, we shall first justify the form of the boundary conditions in (1.2). To do this, consider the linearized KdV equation,

$$\frac{\partial u}{\partial t} + \frac{\partial^3 u}{\partial x^3} = 0. \tag{3.1}$$

Taking Laplace transforms of this equation in t,

$$\frac{\mathrm{d}^3 \bar{u}}{\mathrm{d}x^3} + s\bar{u} = u_\mathrm{i}, \tag{3.2}$$

is obtained, where an overbar denotes the Laplace transform and s is the Laplace transform variable. The solution of (3.2) is

$$\bar{u} = A\mathrm{e}^{\lambda_1 x} + B\mathrm{e}^{\lambda_2 x} + C\mathrm{e}^{\lambda_3 x} + u_\mathrm{i}/s, \tag{3.3}$$

where

$$\lambda_1 = -s^{1/3}, \quad \lambda_2, \quad \lambda_3 = s^{1/3}(\tfrac{1}{2} \pm \mathrm{i}\tfrac{\sqrt{3}}{2}).$$

Two of the roots of the characteristic equation for (3.2) have positive real parts, while the other has a negative real part (see (3.3)). Therefore, if the problem is solved on the positive quarter-plane, boundedness of the solution as $x \to \infty$ implies that $B = C = 0$ and so one boundary condition is needed at $x = 0$ (Marchant & Smyth 1991). On the other hand, if the problem is solved on the negative quarter-plane, then only one boundedness condition must be imposed as $x \to -\infty$, giving $A = 0$. Two boundary conditions are then needed at $x = 0$, as stated in (1.2). The same conclusions regarding the appropriate number of boundary conditions for a well-posed problem for the linear KdV equation are drawn by Fokas (2000) (see theorem (3.1) on p. 4201) and by Chu *et al.* (1983), the latter using an energy conservation argument.

In the present work the special case for which the derivative boundary condition is $u_{\mathrm{b}x} = 0$ will be considered. This is done for simplicity as the solution of transcendental algebraic equations is required when $u_{\mathrm{b}x} \neq 0$, while for $u_{\mathrm{b}x} = 0$ explicit solutions can be found. Moreover, the solutions presented for the case $u_{\mathrm{b}x} = 0$ represent all the qualitatively different solution types which can occur for the negative quarter-plane problem and once the solutions for $u_{\mathrm{b}x} = 0$ have been determined, it will be clear how they can be extended to $u_{\mathrm{b}x} \neq 0$. A further point is that the negative quarter-plane problem (1.2) is formulated in a frame of reference moving with the linear wave speed c_0. On the infinite line this does not matter as there is a simple Galilean transformation which takes solutions back to the physical frame of reference. For quarter-plane problems, however, this Galilean transformation results in the boundary at $x = 0$ becoming a moving boundary with velocity $-c_0$. This does not present a problem, however, as the solutions found here for a fixed boundary can be simply extended to a boundary moving with a constant velocity, as will be clear once these solutions are derived.

(*a*) *Positive* u_{b}

Let us first consider positive boundary values u_{b}. The soliton solution (2.4) can be made steady by taking $\beta = -2a/3$. Then satisfying the boundary conditions at $x = 0$ in the initial boundary-value problem (1.2), we obtain

$$u = -\tfrac{1}{2}u_{\mathrm{b}} + \tfrac{3}{2}u_{\mathrm{b}} \operatorname{sech}^2 \tfrac{1}{2}\sqrt{3u_{\mathrm{b}}}x. \tag{3.4}$$

Now as $x \to -\infty$, $u \to -u_{\mathrm{b}}/2$, so this solution will not satisfy the initial condition in (1.2). To satisfy this initial condition, we now match this steady solution onto a transient front. For $u_{\mathrm{i}} \leqslant -u_{\mathrm{b}}/2$, we have a step down in mean height, so the appropriate transient front is the mean height variation (2.9) with $A = -u_{\mathrm{b}}/2$ and $B = u_{\mathrm{i}}$. Therefore, for $u_{\mathrm{b}} \geqslant 0$ and $u_{\mathrm{i}} \leqslant -u_{\mathrm{b}}/2$, the solution of the negative quarter-plane problem is (3.4) for $-3u_{\mathrm{b}}t \leqslant x \leqslant 0$ and (2.9) for $6u_{\mathrm{i}}t \leqslant x < -3u_{\mathrm{b}}t$, with $u = u_{\mathrm{i}}$ for $x < 6u_{\mathrm{i}}t$. It can be seen that for the front to move backwards, we require $u_{\mathrm{b}} \geqslant 0$.

On the other hand, if $u_{\mathrm{i}} > -u_{\mathrm{b}}/2$, we have a step up in mean height, so the appropriate solution for the transient front is the undular bore solution (2.7) with $A = -u_{\mathrm{b}}/2$ and $B = u_{\mathrm{i}}$. From (2.8) the bore ranges as follows,

$$-6(u_{\mathrm{b}} + u_{\mathrm{i}})t \leqslant x \leqslant (4u_{\mathrm{i}} - u_{\mathrm{b}})t, \tag{3.5}$$

since $m = 1$ at the leading edge and $m = 0$ at the trailing edge of the bore. From the leading edge of (3.5), it can be seen that for the transient front to propagate into $x < 0$ we require $4u_\mathrm{i} < u_\mathrm{b}$. The solution of the negative quarter-plane problem for $u_\mathrm{b} \geqslant 0$ and $-u_\mathrm{b}/2 < u_\mathrm{i} < u_\mathrm{b}/4$ is then (3.4) for $(4u_\mathrm{i} - u_\mathrm{b})t \leqslant x \leqslant 0$ and the undular bore solution (2.7) for $-6(u_\mathrm{b} + u_\mathrm{i})t \leqslant x < (4u_\mathrm{i} - u_\mathrm{b})t$, with $u = u_\mathrm{i}$ for $x < -6(u_\mathrm{b} + u_\mathrm{i})t$.

For $4u_\mathrm{i} \geqslant u_\mathrm{b}$, the undular bore (2.7) would propagate into $x > 0$, which is clearly not possible. For the positive quarter-plane problem, a partial undular bore occurs in this case (Marchant & Smyth 1991). A partial undular bore is the undular bore solution (2.7) cut off at a value of $m \neq 0$ or $m \neq 1$. This partial bore solution does not occur for the negative quarter-plane problem, as the imposition of a fixed derivative at the boundary does not allow the bore to evolve. Instead, for $4u_\mathrm{i} \geqslant u_\mathrm{b}$ a steady cnoidal wave solution (2.1) forms near the boundary. Let us set a_0, β_0 and m_0 to be the amplitude, mean height and modulus, respectively, of this steady cnoidal wave. The steady cnoidal wave must have zero velocity, so the dispersion relation (2.2) gives

$$3\beta_0 + 2a_0\left(2m_0^{-1} - 1 - \frac{3E(m_0)}{m_0K(m_0)}\right) = 0. \tag{3.6}$$

The boundary condition $u_x = 0$ at $x = 0$ gives $\phi = 0$ or π in the phase (2.2). Taking $\phi = 0$ and applying the boundary condition $u = u_\mathrm{b}$ at $x = 0$ gives

$$u_\mathrm{b} = \beta_0 + 2a_0\left(m_0^{-1} - \frac{E(m_0)}{m_0K(m_0)}\right). \tag{3.7}$$

The mean level of the cnoidal wave is β_0, which is always less than the initial condition u_i. Hence a transient front, consisting of a partial undular bore, must be matched onto the steady cnoidal wave in order to bring the mean level up to u_i and so satisfy the initial condition. This partial undular bore is based on the full bore solution (2.7) and has modulus squared in the range $0 \leqslant m \leqslant m_0$ and increases the mean level from β_0 to the initial value u_i. At the rear of the bore $m = 0$, so that from (2.7) $B = u_\mathrm{i}$. At the front of the bore, which matches onto the steady cnoidal wavetrain, the modulus squared $m = m_0$ and the wave amplitude is $a_0 = (u_\mathrm{i} - A)m_0$ from (2.7). Also, at the front of the partial undular bore, the mean level (2.7) must be that of the steady cnoidal wavetrain, giving

$$\beta_0 = (u_\mathrm{i} - A)m_0 + 2A - u_\mathrm{i} + 2(u_\mathrm{i} - A)P(m_0). \tag{3.8}$$

Solving (3.6)–(3.8) gives

$$A = u_\mathrm{i} + \frac{u_\mathrm{i} - u_\mathrm{b}}{m_0}, \tag{3.9}$$

which completes the solution for the partial undular bore and the modulus, amplitude and mean-level of the steady cnoidal wavetrain are then

$$m_0 = \frac{2(u_\mathrm{b} - u_\mathrm{i})}{u_\mathrm{b} + 2u_\mathrm{i}}, \qquad a_0 = u_\mathrm{b} - u_\mathrm{i}, \qquad \beta_0 = u_\mathrm{i} + \frac{a_0}{m_0}(m_0 - 2 + 2P(m_0)). \tag{3.10}$$

This solution is valid for $u_\mathrm{b}/4 \leqslant u_\mathrm{i} \leqslant u_\mathrm{b}$, which gives the modulus squared of the steady cnoidal wave in the range $0 \leqslant m_0 \leqslant 1$. The partial undular bore is (2.7) with $0 \leqslant m \leqslant m_0$, $B = u_\mathrm{i}$ and A given by (3.9) and extends in the range

$$6\left(u_\mathrm{i} - 2\frac{a_0}{m_0}\right)t < x < r_\mathrm{f}t, \tag{3.11}$$

where

$$r_{\mathrm{f}} = 6u_{\mathrm{i}} + 2a_0 - 4a_0 m_0^{-1} - \frac{4a_0(1-m_0)}{P(m_0)-(1-m_0)}.$$

For $r_{\mathrm{f}}t \leqslant x \leqslant 0$ the solution is the steady cnoidal wave of modulus squared m_0, amplitude a_0 and mean height β_0. For $6(u_{\mathrm{i}} - 2a_0/m_0)t \leqslant x \leqslant r_{\mathrm{f}}t$ the solution is the partial undular bore (2.7), while for $x \leqslant 6(u_{\mathrm{i}} - 2a_0/m_0)t$ the solution is $u = u_{\mathrm{i}}$.

For the case $u_{\mathrm{i}} > u_{\mathrm{b}}$ we must take $\phi = \pi$ to satisfy the boundary condition $u_x = 0$ at $x = 0$. Then in a similar manner to the determination of the parameters for $\phi = 0$, it is found that the amplitude and modulus squared of the steady cnoidal wavetrain are given by

$$m_0 = \frac{2(u_{\mathrm{i}} - u_{\mathrm{b}})}{4u_{\mathrm{i}} - u_{\mathrm{b}}} \quad \text{and} \quad a_0 = u_{\mathrm{i}} - u_{\mathrm{b}}. \tag{3.12}$$

The mean height is again given by the third of (3.10) and the extent of the partial undular bore by (3.11). In this case the modulus squared of the steady cnoidal wave ranges between $0 \leqslant m_0 \leqslant 0.5$. The partial undular bore which forms the front of the steady cnoidal wave is given by (2.7) with $0 \leqslant m \leqslant m_0$, $B = u_{\mathrm{i}}$ and

$$A = u_{\mathrm{i}} - \frac{u_{\mathrm{i}} - u_{\mathrm{b}}}{m_0}. \tag{3.13}$$

Ahead of this front, again $u = u_{\mathrm{i}}$. This then completes the determination of the solutions of the initial boundary-value problem in the parameter space $(u_{\mathrm{i}}, u_{\mathrm{b}})$ for positive u_{b}.

(*b*) *Negative* u_{b}

Let us now consider negative boundary values u_{b}. The solutions of the negative quarter-plane problem in this case are determined in a similar manner as in the previous subsection for positive u_{b}, so only the basic details of the determination of these solutions will be given.

Again taking the soliton solution (2.4) to be steady, we have $\beta = -2a/3$. Then satisfying the boundary condition $u_x = 0$ at $x = 0$ gives $\phi = \infty$, so that the solution is the uniform shelf

$$u = u_{\mathrm{b}}. \tag{3.14}$$

This solution will be preceded by a transient front in order to match to the initial condition. For $u_{\mathrm{i}} \leqslant u_{\mathrm{b}}$, we have a step down in mean height, so that the appropriate transient front is the mean height variation (2.9) with $A = u_{\mathrm{b}}$ and $B = u_{\mathrm{i}}$. The solution of the negative quarter-plane problem for $u_{\mathrm{b}} < 0$ and $u_{\mathrm{i}} \leqslant u_{\mathrm{b}}$ is therefore (3.14) for $6u_{\mathrm{b}}t \leqslant x \leqslant 0$, (2.9) for $6u_{\mathrm{i}}t \leqslant x < 6u_{\mathrm{b}}t$ and $u = u_{\mathrm{i}}$ for $x < 6u_{\mathrm{i}}t$ to match with the initial condition.

On the other hand, when $u_{\mathrm{i}} > u_{\mathrm{b}}$, there is a step up in mean height and the transient front is given by the undular bore solution (2.7) with $A = u_{\mathrm{b}}$ and $B = u_{\mathrm{i}}$. At the leading edge of the bore $m = 1$ and at its trailing edge $m = 0$. Therefore, from (2.8), the bore extends in the range

$$6(2u_{\mathrm{b}} - u_{\mathrm{i}})t \leqslant x \leqslant 2(u_{\mathrm{b}} + 2u_{\mathrm{i}})t. \tag{3.15}$$

Now the bore must propagate into the region $x < 0$. Therefore, from the velocity of the leading edge of (3.15), we see that we require $u_{\mathrm{i}} < -u_{\mathrm{b}}/2$. So summing up,

Table 1. *Summary of parameter regions*

	mean height variation	undular bore
uniform shelf	$u_\mathrm{i} \leqslant u_\mathrm{b} \leqslant 0$	$u_\mathrm{b} \leqslant u_\mathrm{i} \leqslant -\frac{1}{2}u_\mathrm{b}$
sech^2 profile	$0 \leqslant u_\mathrm{b} \leqslant -2u_\mathrm{i}$	$-\frac{1}{2}u_\mathrm{b} \leqslant u_\mathrm{i} \leqslant \frac{1}{4}u_\mathrm{b}$
cnoidal wave		$-2u_\mathrm{i} \leqslant u_\mathrm{b} \leqslant 4u_\mathrm{i}$

we have that the solution of the negative quarter-plane problem for $u_\mathrm{b} < 0$ and $u_\mathrm{b} < u_\mathrm{i} < -u_\mathrm{b}/2$ is $u = u_\mathrm{b}$ for $2(u_\mathrm{b} + 2u_\mathrm{i})t \leqslant x \leqslant 0$, the undular bore solution (2.7) with $A = u_\mathrm{b}$ and $B = u_\mathrm{i}$ as a transient front in $6(2u_\mathrm{b} - u_\mathrm{i})t < x < 2(u_\mathrm{b} + 2u_\mathrm{i})t$ and $u = u_\mathrm{i}$ for $x \leqslant 6(2u_\mathrm{b} - u_\mathrm{i})t$ to match with the initial condition.

The final portion of the parameter space $(u_\mathrm{i}, u_\mathrm{b})$ for $u_\mathrm{b} < 0$ is $u_\mathrm{i} > -u_\mathrm{b}/2$, for which the leading edge of the undular bore solution (2.7) would propagate into $x > 0$. As in the mirror case for positive u_b, the solution in this regime is a steady cnoidal wave of the form (2.1) matched to a partial undular bore. The parameters of this steady cnoidal wave are given by (3.12), but in this case the cnoidal wavetrain has modulus $0.5 \leqslant m_0 \leqslant 1$. This completes the solutions of the negative quarter-plane problem for negative u_b.

As a summary, the regions of the $(u_\mathrm{i}, u_\mathrm{b})$ parameter space in which the five different types of solutions of the negative quarter-plane problem occur are listed in table 1.

4. Results and discussion

In this section the approximate solutions found in § 3 will be compared with numerical solutions for the negative quarter-plane problem (1.2). The boundary values u_b and initial values u_i were chosen so that each of the five different solution types, as summarized in table 1, were obtained. The numerical solutions of the present work were found using a hybrid Runge–Kutta finite-difference scheme, which is described in the appendix. The parameters used in the numerical scheme were $\Delta x = 0.1$ and $\Delta t = 1 \times 10^{-3}$. Numerical solutions were obtained for different values of Δx and Richardson extrapolation was then used to estimate the accuracy of these solutions. It was found that the maximum error, in all the presented solutions, was less than 1%. The largest errors typically occurred at the peaks of the cnoidal waves with large amplitude.

Figure 1 shows the free-surface elevation u versus $-x$ at $t = 20$ for the parameters $u_\mathrm{i} = -0.5$ and $u_\mathrm{b} = 0.5$. The approximate solution consists of three main portions, as outlined in the previous section and summarized in table 1. Next to the boundary, for $0 < -x < 30$, the steady-state sech^2 profile occurs. This takes the solution from the boundary value $u = u_\mathrm{b} = 0.5$ to the level of the uniform shelf $u = -u_\mathrm{b}/2 = -0.25$. The solution for $30 < -x < 60$ then consists of a mean height variation, while for $-x > 60$ it is the initial value $u = u_\mathrm{i} = -0.5$. The comparison with the numerical solution is excellent, with the differences between the solutions seen in the figure easily explained. Firstly, for $-x > 60$ the numerical solution consists of a train of small amplitude waves with mean level $u = u_\mathrm{i}$. These waves are due to the dispersive smoothing of the discontinuities in u_x at the edges $x = 6At$ and $x = 6Bt$ of the mean height variation (Fornberg & Whitham 1978). The mean level variation solution (2.9)

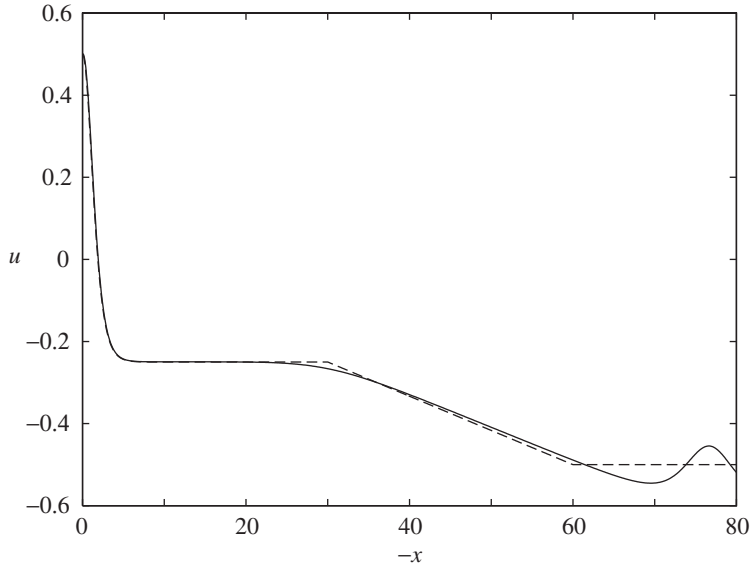

Figure 1. The free-surface elevation u versus $-x$ at $t = 20$ for the parameters $u_\mathrm{i} = -0.5$ and $u_\mathrm{b} = 0.5$. Shown are the approximate (dashed) and numerical (solid) solutions of (1.2). The approximate solution consists of a sech^2 profile for $0 < -x < 30$, a mean height variation for $30 < -x < 60$ and the initial value $u = -0.5$ for $-x > 60$.

neglects these small amplitude waves. In this regard it is noted that these small amplitude waves propagate to $x = -\infty$ as time increases.

Figure 2 shows the free-surface elevation u versus $-x$ at $t = 20$ for the parameters $u_\mathrm{i} = -1$ and $u_\mathrm{b} = -0.5$. For these initial and boundary conditions, it is seen from table 1 that the analytical solution consists of a steady shelf near the boundary and a mean height variation. This solution is qualitatively similar to the solution shown in figure 1, since the shelf is a limiting case of the steady sech^2 profile. The shelf extends from $x = 0$ out to $x = -60$ at the level u_b. A mean height variation then occurs for $60 < -x < 120$, taking the solution down to the initial value $u = u_\mathrm{i} = -1$. As for figure 1, there is excellent agreement between the numerical and approximate solutions. Again the numerical solution has a small amplitude wavetrain ahead of the mean height variation. This wave train is due to the dispersive resolution of the discontinuities in u_x at its ends, as for the numerical solution shown in figure 1.

Figure 3 shows the free-surface elevation u versus $-x$ at $t = 20$ for the parameters $u_\mathrm{i} = 0$ and $u_\mathrm{b} = 1$. For these initial and boundary values, table 1 shows that the analytical solution consists of the steady sech^2 profile and the undular bore solution as a front. The solution is then the sech^2 profile for $0 < -x < 20$, which takes the solution from the boundary level $u = u_\mathrm{b} = 1$ to a shelf of height $u = -u_\mathrm{b}/2 = -0.5$. Linking the level at the end of the shelf to the initial value $u = u_\mathrm{i} = 0$ is the undular bore solution. This undular bore solution consists of a modulated cnoidal wave with modulus squared m which varies through the bore. At the leading edge, at $x = -20$, the modulus squared is $m = 1$, so from (2.7) the leading edge of the bore consists of solitons of amplitude unity on a mean level $\beta = -0.5$. At the trailing edge, at $x = -120$, the modulus squared is $m = 0$, so that the trailing edge of the bore consists of linear (small amplitude) waves on a mean level $\beta = 0$. The undular

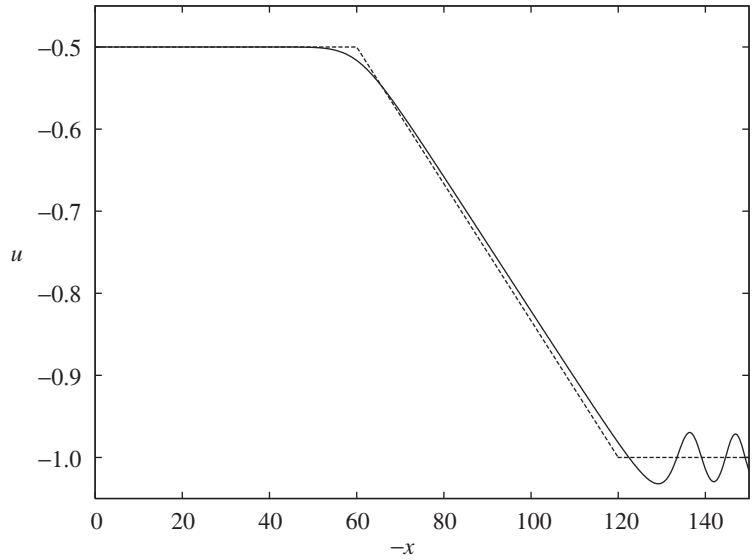

Figure 2. The free-surface elevation u versus $-x$ at $t = 20$ for the parameters $u_{\mathrm{i}} = -1$ and $u_{\mathrm{b}} = -0.5$. Shown are the approximate (dashed) and numerical (solid) solutions of (1.2). The approximate solution consists of a uniform shelf for $0 < -x < 60$, a mean height variation for $60 < -x < 120$ and the initial value $u = -1$ for $-x > 120$.

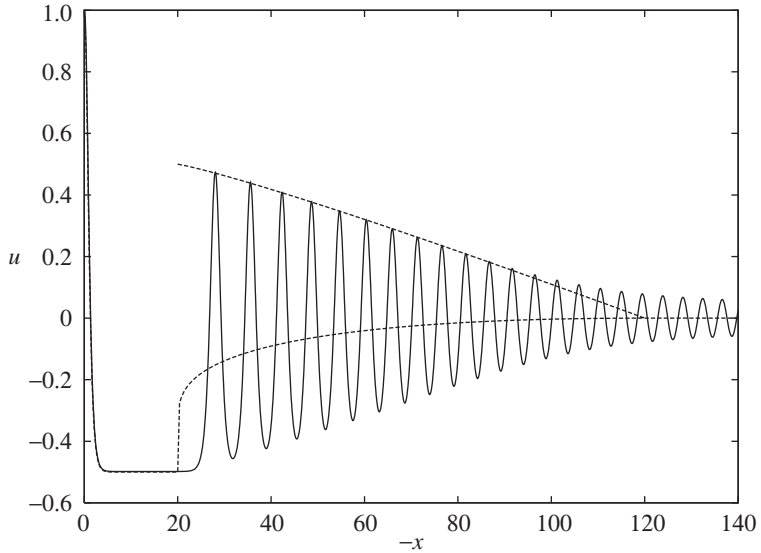

Figure 3. The free-surface elevation u versus $-x$ at $t = 20$ for the parameters $u_{\mathrm{i}} = 0$ and $u_{\mathrm{b}} = 1$. Shown are the approximate (dashed) and numerical (solid) solutions of (1.2). The approximate solution consists of a sech^2 profile for $0 < -x < 20$, an undular bore for $20 < -x < 120$ and the initial value $u = 0$ for $-x > 120$. For the approximate undular bore, the averaged quantities of the mean height and wave envelope are shown.

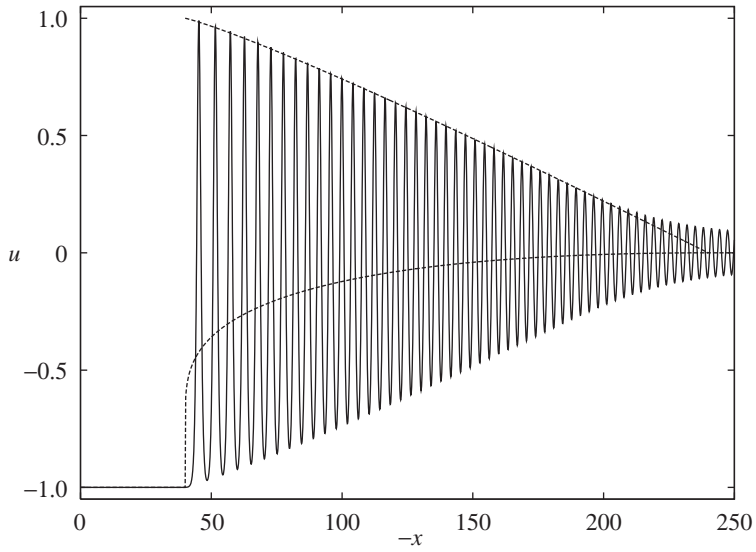

Figure 4. The free-surface elevation u versus $-x$ at $t = 20$ for the parameters $u_\mathrm{i} = 0$ and $u_\mathrm{b} = -1$. Shown are the approximate (dashed) and numerical (solid) solutions of (1.2). The approximate solution consists of a uniform shelf for $0 < -x < 40$, an undular bore for $40 < -x < 240$ and the initial value $u = 0$ for $-x > 240$. For the approximate undular bore, the averaged quantities of the mean height and wave envelope are shown.

bore solution (2.7) and (2.8) for the front provides averaged information, such as the mean level and the envelope of the wavetrain. For this reason, in figure 3 the mean level, β, and the wave envelope, $\beta + 2am^{-1}(1 - P(m))$, are plotted for the analytical solution in the region of the undular bore. It can be seen that the wave envelope gives an excellent comparison with the numerical solution throughout the bore. For $-x > 120$ the numerical solution consists of linear (small amplitude) waves on a mean level $u = u_\mathrm{i}$, these waves propagating to $x = -\infty$ as time increases.

Figure 4 shows the free-surface elevation u versus $-x$ at $t = 20$ for the parameters $u_\mathrm{i} = 0$ and $u_\mathrm{b} = -1$. Table 1 shows that the analytical solution for these initial and boundary values consists of a steady shelf at the boundary preceded by an undular bore taking the solution to the initial value. As for figure 3, in the region of the undular bore the mean level and wave envelope of the analytical solution are shown. The solution is qualitatively similar to that shown in figure 3: a steady shelf of mean level $u = u_\mathrm{b} = -1$ extends to $x = -40$ and then an undular bore links this level to the initial level $u = u_\mathrm{i}$ at $x = -240$. Again an excellent comparison is obtained between the numerical and analytical solutions.

Figures 5 and 6 shows the free-surface elevation u versus $-x$ at $t = 20$ for the parameters $u_\mathrm{i} = 1$ and $u_\mathrm{b} = 0$. For this choice of initial and boundary values table 1 shows that the analytical solution consists of a steady cnoidal wavetrain at the boundary and a partial undular bore which brings the solution up to the mean level. The steady cnoidal wave has modulus squared $m_0 = 0.5$, an amplitude $a_0 = 1$ and a mean level $\beta_0 = 0.914$. The wavelength is $\lambda_0 = 2.40$. Further the steady cnoidal wave has a minimum value of $u = 0$ and a maximum value of $u = 2$ and extends from the boundary to $x = -175$. The partial undular bore extends between $175 < -x < 356$ and links the mean level $\beta_0 = 0.914$ at $x = -175$ to the initial level $u = u_\mathrm{i} = 1$

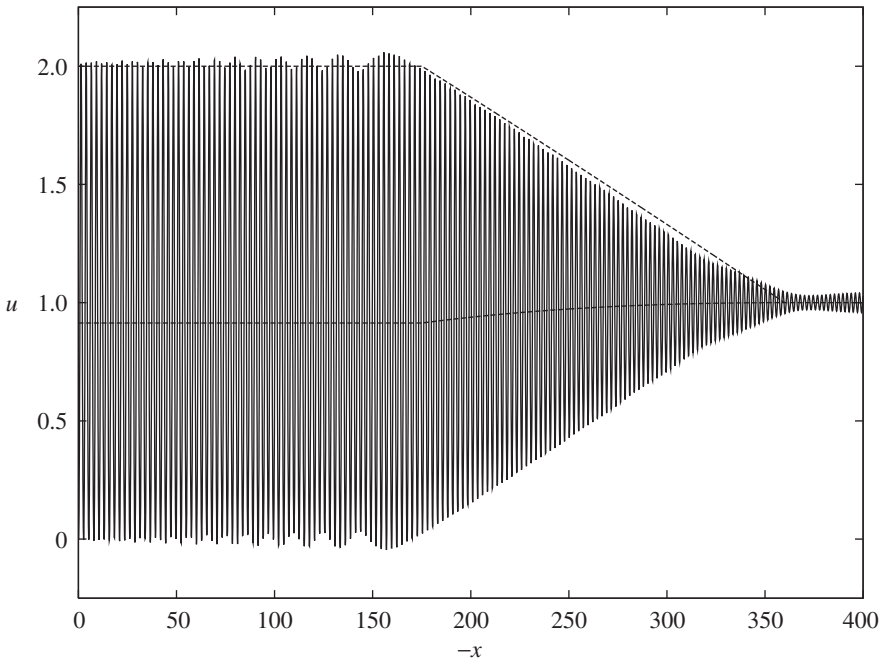

Figure 5. The free-surface elevation u versus $-x$ at $t = 20$ for the parameters $u_{\mathrm{i}} = 1$ and $u_{\mathrm{b}} = 0$. Shown are the approximate (dashed) and numerical (solid) solutions of (1.2). The approximate solution consists of a steady cnoidal wave for $0 < -x < 170$, a partial undular bore for $170 < -x < 356$ and the initial value $u = 1$ for $-x > 356$. For the approximate solution, the averaged quantities of the mean height and wave envelope are shown.

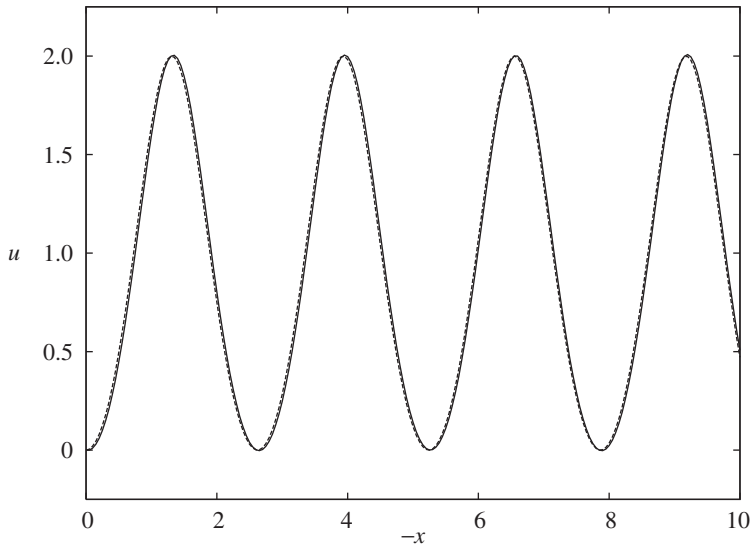

Figure 6. The free-surface elevation u versus $-x$ at $t = 20$ for the parameters $u_{\mathrm{i}} = 1$ and $u_{\mathrm{b}} = 0$. For the region displayed, the solution is a steady cnoidal wave. Shown are the approximate (dashed) and numerical (solid) solutions of (1.2).

at $x = -356$. In figure 5 both the mean level and wave envelope are plotted. An excellent comparison between the numerical solution and the analytical wave envelope is obtained, both for the steady cnoidal wavetrain and the partial undular bore. Some small oscillations in amplitude can be seen in the steady cnoidal wavetrain. These oscillations are produced at the boundary during the initial evolution of the wavetrain and are associated with the discretization of the initial discontinuity in u. They propagate to infinity at large times. Beyond the undular bore, for $-x > 356$, the numerical solution shows small amplitude waves on a mean level $u = u_{\mathrm{i}} = 1$. A detailed comparison for the steady cnoidal wave at the boundary is made in figure 6 and again the comparison is excellent.

5. Summary

Five qualitatively different types of approximate solutions of the negative quarter-plane problem (1.2) are derived, the particular solution depending on the relation between the initial and boundary values. A good comparison is obtained between all these approximate solutions and numerical solutions of the initial boundary-value problem (1.2). A key feature of the problem is the choice of boundary conditions; it is shown that the appropriate boundary conditions are different for the positive and negative quarter-plane problems. The techniques presented here for developing approximate solutions are simple and directly motivated by the physics of the problem. They should prove useful for solving initial boundary-value problems for other nonlinear dispersive wave equations, such as the Boussinesq equations, the modified KdV equation and the Benjamin–Ono equation.

Appendix A. The numerical scheme

The numerical solutions of the KdV equation are obtained by using centred finite-differences in the spatial coordinate x and a fourth-order Runge–Kutta method for the temporal coordinate t. This method was chosen over straight finite-difference methods, such as the finite-difference scheme of Zabusky & Kruskal (1965), because of its stability. Given that the solution at time t_k is

$$u_{k,j} = u(t_k = k\Delta t, x_j = -j\Delta x), \quad j = 0, \ldots, N, \tag{A 1}$$

the solution at time t_{k+1} is given by

$$u_{k+1,j} = u_{k,j} + \tfrac{1}{6}(a_{k,j} + 2b_{k,j} + 2c_{k,j} + d_{k,j}), \qquad j = 1, \ldots, N, \tag{A 2}$$

where

$$\begin{aligned} a_{k,j} &= \Delta t f(\eta_{k,j}), & b_{k,j} &= \Delta t f(\eta_{k,j} + \tfrac{1}{2}a_{k,j}),\\ c_{k,j} &= \Delta t f(\eta_{k,j} + \tfrac{1}{2}b_{k,j}), & d_{k,j} &= \Delta t f(\eta_{k,j} + c_{k,j}). \end{aligned}$$

The function f is the finite-differenced form of all the terms in the KdV equation involving spatial derivatives,

$$\left.\begin{aligned} f(p_{k,j}) = &-\frac{3p_{k,j}}{\Delta x}(p_{k,j+1} - p_{k,j-1})\\ &- \frac{1}{2\Delta x^3}(p_{k,j+2} - 2p_{k,j+1} + 2p_{k,j-1} - p_{k,j-2}), \quad j = 2, \ldots, N,\\ f(p_{k,0}) = f(p_{k,1}) &= 0. \end{aligned}\right\} \tag{A 3}$$

Near the boundary, for $j = 0, 1$, the function $f = 0$ as the solution is given by the boundary conditions. The boundary and initial conditions used are

$$u_{0,j} = u_{\mathrm{i}}, \quad j \geqslant 2, \qquad u(k,0) = u_{\mathrm{b}}, \quad u(k,1) = u_{\mathrm{b}} + \Delta x u_{\mathrm{b}x}, \quad \forall k. \tag{A 4}$$

The boundary condition maintains the appropriate conditions at $x = 0$ and as $x \to -\infty$. The accuracy of the numerical method at each time-step is $O(\Delta t^4, \Delta x^2)$.

References

Camassa, R. & Wu, T. Y. 1989 The Korteweg–de Vries equation with boundary forcing. *Wave Motion* **11**, 495–506.

Chu, X.-L., Xiang, L. W. & Baransky, Y. 1983 Solitary waves induced by boundary motion. *Commun. Pure Appl. Math.* **36**, 495–504.

Clarke, S. R. & Imberger, J. 1994 Nonlinear effects in the unsteady, critical withdrawal of a stratified fluid. In *Fourth Int. Symp. on Stratified Flows*, 29 June–2 July 1994, Grenoble, France, pp. 1–8. Grenoble: Laboratoire des Ecoulements Géophysiques et Industriels.

Fokas, A. S. 1997 A unified transform method for solving linear and certain nonlinear PDEs. *Proc. R. Soc. Lond.* A **453**, 1411–1443.

Fokas, A. S. 2000 On the integrability of linear and nonlinear partial differential equations. *J. Math. Phys.* **41**, 4188–4237.

Fokas, A. S. & Ablowitz, M. J. 1989 Forced nonlinear evolution equations and the inverse scattering transform. *Stud. Appl. Math.* **80**, 253–272.

Fokas, A. S. & Pelloni, B. 1998 The solution of certain initial boundary-value problems for the linearized Korteweg–de Vries equation. *Proc. R. Soc. Lond.* A **454**, 645–657.

Fokas, A. S. & Pelloni, B. 2000 Method for solving moving boundary value problems for linear evolution equations. *Phys. Rev. Lett.* **84**, 4785–4789.

Fornberg, B. & Whitham, G. B. 1978 A numerical and theoretical study of certain nonlinear wave phenomena. *Phil. Trans. R. Soc. Lond.* A **289**, 373–403.

Gardner, C. S., Green, J. M., Kruskal, M. D. & Miura, R. M. 1967 Method for solving the Korteweg–de Vries equation. *Phys. Rev. Lett.* **19**, 1095–1098.

Gurevich, A. V. & Pitaevskii, L. P. 1974 Nonstationary structure of a collisionless shock wave. *Sov. Phys. JETP* **33**, 291–297.

Hirota, R. 1972 Exact solution of the Korteweg–de Vries equation for multiple collisions of solitons. *Phys. Rev. Lett.* **27**, 1192–1194.

Kichenassamy, S. & Olver, P. J. 1992 Existence and nonexistence of solitary wave solutions to higher-order model evolution equations. *SIAM J. Math. Analysis* **23**, 1141–1166.

Marchant, T. R. & Smyth, N. F. 1991 Initial-boundary value problems for the Korteweg–de Vries equation. *IMA J. Appl. Math.* **47**, 247–264.

Whitham, G. B. 1965 Nonlinear dispersive waves. *Proc. R. Soc. Lond.* A **283**, 238–261.

Whitham, G. B. 1974 *Linear and nonlinear waves*. Wiley.

Zabusky, N. J. & Kruskal, M. D. 1965 Interaction of solitons in a collisionless plasma and the recurrence of initial states. *Phys. Rev. Lett.* **15**, 240–243.